Retrieval of effective radius and liquid water path from ground-based instruments: A case study at Barrow, Alaska

Robyn Schofield,[1,2,3] John S. Daniel,[1] Robert W. Portmann,[1] H. LeRoy Miller,[1,2]
Susan Solomon,[1] Charles S. Eubank,[1,2] Megan L. Melamed,[1,2] Andrew O. Langford,[1]
Matthew D. Shupe,[2,4] and David D. Turner[5]

[1]   Two methods for retrieving cloud droplet effective radius r_e from ground-based near-infrared spectral measurements of path-integrated liquid water paths (PLWPs) are described. In one method the PLWP is compared with column measurements of liquid water path (LWP) from a dual channel microwave radiometer (MWR) to estimate the cloud path enhancement, which is then used to derive the cloud droplet effective radius. In the second method, PLWP is combined with absolutely calibrated zenith radiances at 500 nm to retrieve r_e and LWP simultaneously. Both techniques are used in a case study of marine stratocumulus at the Barrow, Alaska (71.32°N, 156.62°W) Atmospheric Radiation Measurement Program (ARM) site on 17 September 2004. The first method performed best for moderately thick clouds (LWP $\geq$ 100 g m^{-2}), but the accuracy is limited by uncertainties in the MWR LWP on which it relies. The second method performed well over a wider range of values with 1σ retrieval errors of <4 g m^{-2} (~4%) and ~3 μm (~7%) for 15 $\leq$ LWP $\leq$ 170 g m^{-2}. The LWPs retrieved using the radiance-PLWP method were highly correlated (r^2 = 0.96) with LWPs from the MWR (with a bias subtracted) derived using the ARM statistical method. A limited comparison (LWP < 100 g m^{-2}) to millimeter wave cloud radar showed that values of r_e retrieved using the radiance-PLWP method were consistently higher (by ~3 μm) than the LWC-weighted mean r_e from the radar. Additional field studies are needed to resolve this discrepancy, although this first comparison is promising.

Citation: Schofield, R., J. S. Daniel, R. W. Portmann, H. L. Miller, S. Solomon, C. S. Eubank, M. L. Melamed, A. O. Langford, M. D. Shupe, and D. D. Turner (2007), Retrieval of effective radius and liquid water path from ground-based instruments: A case study at Barrow, Alaska, *J. Geophys. Res.*, *112*, D21203, doi:10.1029/2007JD008737.

1. Introduction

[2]   Clouds are recognized as the dominant contributor to the Earth's global albedo and thus play an important role in the Earth's climate system. Marine boundary layer clouds, in particular, have a large impact on climate since they are present on average more than 40% of the time over the world's oceans and coastal regions [*Warren et al.*, 1985]. These clouds generally cool the surface since they have visible albedos much larger than the underlying ocean and emit IR radiation at warmer temperatures than higher clouds. *Charlson et al.* [1992] noted that an increase of 0.03 in the marine stratus albedo would lead to a global mean forcing of −1.8 W m^{-2}. Such a change in albedo could arise from an increase in cloud cover or from a decrease in the effective cloud drop radius (r_e) due to the first aerosol indirect effect. This effect, as described by *Twomey* [1974], refers to the process by which increasing aerosol levels can lead to a larger cloud droplet number density (N), and thus smaller r_e, for a given liquid water content (LWC).

[3]   Aerosol indirect effects on clouds are currently among the most uncertain processes within climate models [*Intergovernmental Panel on Climate Change*, 2001]. One way to quantify the first indirect effect is to combine aerosol measurements with measurements of any two of the inter-dependent cloud parameters: r_e, N, or LWC (or its vertical integral liquid water path (LWP)) [*Kim et al.*, 2003; *Garrett et al.*, 2004; *Feingold et al.*, 2006] related through the following equation [*Dong and Mace*, 2003a]:

$$r_e = \exp(\sigma_x^2)\left[\frac{3}{4\pi}\frac{\text{LWP}}{\rho_w Nh}\right]^{1/3}, \quad (1)$$

[1]NOAA, Chemical Sciences Division, Earth Systems Research Laboratory, Boulder, Colorado, USA.

[2]Cooperative Institute for Research in Environmental Sciences, University of Colorado, Boulder, Colorado, USA.

[3]Now at the Alfred Wegener Institute for Polar and Marine Research, Potsdam, Germany.

[4]NOAA, Physical Sciences Division, Earth Systems Research Laboratory, Boulder, Colorado, USA.

[5]Space Science and Engineering Center, University of Wisconsin-Madison, Madison, Wisconsin, USA.

where h is the cloud thickness, ρ_w is the density of water, and σ_x is the logarithmic width of the lognormal cloud droplet size distribution spectral dispersion ($r_e = \exp(\sigma_x^2)r_v$ (the volumetric radius)). For unpolluted conditions this logarithmic width is approximately 0.38 [*Han et al.*, 1998; *Dong and Mace*, 2003a; *Boers et al.*, 2006]. For liquid clouds, N can be related to the aerosol concentration via the role that aerosols play as cloud condensation nuclei.

[4] While in situ measurements provide essential information about in-cloud processes and are needed to validate remote-sensing techniques, the latter are best suited for the long-term monitoring of marine boundary layer clouds needed to better quantify the first indirect effect [*Dong and Mace*, 2003a; *Boers et al.*, 2006]. Existing remote-sensing methodologies entail the measurement of r_e and either LWP or τ, the cloud optical depth. Retrievals of these quantities are often highly uncertain, however, this is largely due to the sensitivity to assumptions about the shape and spread of the droplet size distribution, the droplet number density N, and the LWC profile [*Shupe et al.*, 2005; *Boers et al.*, 2006].

[5] Historically, the retrieval of r_e from ground-based remote-sensing instrumentation has relied heavily upon microwave radiometer (MWR) measurements of LWP. Vertical profiles of effective radii for nonprecipitating clouds have been retrieved by combining MWR LWP with millimeter cloud radar (MMCR) reflectivities [*Frisch et al.*, 1998; *Moran et al.*, 1998; *Miles et al.*, 2000; *Shupe et al.*, 2001; *McFarlane et al.*, 2002], and LWC-weighted cloud average effective radii have been retrieved by combining MWR LWP with ground-based MultiFilter Rotating Shadowband Radiometer (MFRSR) irradiance measurements [*Harrison and Michalsky*, 1994; *Harrison et al.*, 1994; *Min and Harrison*, 1996]. For the MFRSR-MWR combined retrieval, biases and errors in the MWR LWP measurements dominate the overall error in the derivation of r_e, especially at small optical depths and at low LWPs [*Min et al.*, 2003]. These errors arise primarily from ambiguities and assumptions (i.e., water vapor absorption model, representativity of radiosonde training data set) in the LWP retrieval [*Crewell and Löhnert*, 2003].

[6] Discrepancies also arise from different sampling volumes and integration times when different types of measurements are combined or compared. *Frisch et al.* [2002] found higher errors in the retrieved r_e for the radar MWR combined retrieval (~19%) relative to the radar only retrieval (~15%) when both methods were compared to in situ measurements. Both the MWR LWP errors and the different fields of view of the MWR and radar instruments were cited as the reason for these higher r_e errors [*Frisch et al.*, 2002; *Shupe et al.*, 2005]. *Feingold et al.* [2006] examined and compared the different sensitivities of these remote ground-based measurements as well as above-cloud remote r_e retrievals at the Southern Great Plains (SGP) Atmospheric Radiation Measurement (ARM) site operated by the U.S. Department of Energy (DOE). They found that the downward viewing remote sensors of the Moderate Resolution Imaging Spectroradiometer satellite [*Gao and Kaufman*, 2003] and the airborne Solar Spectral Flux Radiometer [*Pilewskie et al.*, 2003] observed slightly higher mean radii than the MMCR and MFRSR ground-based instruments because the former preferentially sampled the uppermost

part of the cloud. *Dong and Mace* [2003a] compared MMCR r_e retrievals (with and without MWR LWP constraint) with in situ aircraft measurements in another study at the SGP ARM site and found that it was necessary to use relatively long 30-min averages to obtain a good comparison because of differences in the cloud volumes sampled by the two methodologies. Improved methods for simultaneously determining LWC and r_e are therefore useful to eliminate these sources of uncertainty.

[7] Recently, *Min and Duan* [2005] described a new method that allowed the simultaneous retrieval of r_e and LWP using the angular distribution of the forward scattering lobe of cloud droplets observed with multiple shadowband scans. This new technique, which avoids the MWR LWP and its associated errors, is estimated to produce small errors of 10% for r_e and 2 g m^{-2} for LWP but is applicable only to optically thin clouds. In this paper we describe two additional methodologies based on measurements of the path-integrated liquid water path (PLWP) using a relatively inexpensive ground-based near-infrared (NIR) spectrometer. The first method, suggested by *Daniel et al.* [2006], combines the PLWP with colocated MWR LWP measurements to retrieve r_e (this method is hereafter referred to as MWR-PLWP). The second method, applicable to a wide range of cloud optical thicknesses, retrieves r_e and LWP by combining the PLWP measurements with absolutely calibrated radiance measurements at 500 nm (this method is hereafter referred to as Rad$_{500}$-PLWP). Since this retrieval does not use the MWR LWP, complications related to combining distinct instruments, such as the different field of view, cloud sample volumes, and temporal sampling, are avoided. We note that this second method is, in principle, similar to the MFRSR MWR retrievals, described by *Harrison and Michalsky* [1994] and *Min and Harrison* [1996], with radiance replacing irradiance and PLWP replacing LWP in the retrieval.

[8] The NIR PLWP, 500 nm radiance, and MWR LWP measurement techniques are described in section 2. Section 3 presents a case study using measurements of marine boundary layer clouds made on 17 September 2004 at the Barrow, Alaska (71.32°N 156.62°W) Atmospheric Radiation Measurement (ARM) site operated by the DOE to evaluate the two retrieval methods for obtaining r_e (MWR-PLWP) and for obtaining r_e and LWP (Rad$_{500}$-PLWP). Section 4 discusses errors in the retrieved r_e and LWP derived from the observational uncertainties for both methodologies, and the retrieved radii are compared with radii estimated from MMCR under nondrizzle conditions. The retrieval errors resulting from modeling assumptions are also examined, and the independent pieces of information that can be derived from the measurements (degrees of freedom for signal) characterizing the retrievals of r_e and LWP are determined. In section 5 the relative merits of these two approaches and other measurement techniques are discussed.

2. Measurement Techniques

[9] The NIR spectral measurements were made with a commercially available Czerny-Turner spectrometer with an InGaAs detector cooled to $-10°C$. The spectrometer covers the wavelength range from 0.9 to 1.7 μm with a full width at

half maximum (FWHM) resolution of ~0.005 μm. Light scattered from the zenith sky was collected by an optical fiber and coupled into the laboratory-based spectrometer (see below). The spectral data were acquired with a 2-s integration time. This instrument has been described in more detail elsewhere [*Langford et al.*, 2005; *Daniel et al.*, 2006].

[10] The spectra were analyzed using a variant of the differential optical absorption spectroscopy (DOAS) technique [see, e.g., *Noxon*, 1975; *Platt*, 1994]. By fitting the ratio of two zenith-sky spectra to an appropriate set of reference spectra the path-integrated amounts of liquid water and ice can be determined. The use of ratios largely cancels out the effects of instrumental response and solar features on the analysis and much of the absorption due to water vapor. The weakly structured liquid water absorption features are distinguished from the much broader features of aerosol and Rayleigh extinction by including a set of smoothly varying terms along with the reference cross sections. In contrast to most DOAS applications we fit the ratio rather than the natural logarithm of the ratio. This was necessary as liquid water and water vapor are optically thick absorbers implying that Beer's law cannot be applied by simply taking the slant column difference between the foreground and background spectra (see *Daniel et al.* [2006] for details).

[11] The fitting was achieved using an optimal estimation scheme with a basis set of temperature-dependent water and ice absorption cross sections as detailed by *Daniel et al.* [2006]. This permits the retrieval of PLWP, path-integrated ice water path (PIWP), liquid and ice temperatures, and photon path distribution. A liquid water cross section, linearly interpolated for the relevant temperature between -8 and $22°C$ [*Kou et al.*, 1993], was used to derive the PLWP. Since all of the liquid absorption occurs within the droplets, the amount of absorption does not depend upon the distance between the water droplets but rather upon the number and absorption efficiency of the scattering events the photons undergo in their path through the cloud to the ground-based detector. The quantity of liquid outside the cloud (contained within a few large droplets) is generally negligible relative to the liquid within the cloud so that the PLWP measurements should be minimally affected by drizzle (MWR LWP measurements were also not appreciably influenced by drizzle [*Kim et al.*, 2003]). For the measurements described here, the liquid and ice temperatures and path distribution were fixed and the PIWP set to zero.

[12] The zenith-sky radiance was measured with a commercially available silicon photodiode (blue enhanced photovoltaic Type PDB-V108). A bandpass filter (f10-500-4 CVI) was used to selectively accept light centered at 500 nm with a FWHM of 10 nm. The photodiode was illuminated by one leg of a 7-leg branched fiber with a common end at the zenith-viewing port (the NIR spectrometer was fed by one of the other legs). The optics of the common viewing port restricted both measurements to the same 10° full angle field. The photodiode was calibrated in the field using a National Institute of Standards and Technology traceable lamp to yield absolute radiances.

[13] The ARM MWR LWP products are derived using dual channel passive microwave radiometers with a long history of remotely sensing atmospheric water vapor and liquid phase column amounts [*Westwater*, 1978; *Hogg et al.*, 1983]. The MWR LWP retrieval uses measurements at two frequencies of 23.8 and 31.4 GHz [*Westwater*, 1993; *Morris*, 2006]. The MWR located at Barrow, Alaska, has a field of view of 5.9° for the 23.8 GHz channel and 4.5° for the 31.4 GHz channel. The ARM LWP is reported at a temporal resolution of 20 s and is derived using a statistical methodology [*Liljegren and Lesht*, 1996; *Morris*, 2006]. If the conditions of a particular case study vary greatly from the monthly mean, then a bias can be introduced. An error of 20 g m^{-2} and a bias of 15–30 g m^{-2} is found in the LWPs retrieved using different methods [*Crewell and Löhnert*, 2003; *Marchand et al.*, 2003].

3. Observations and Analysis

[14] A case study of the coastal marine boundary layer stratus clouds near Barrow, Alaska is used to illustrate the two methods for radii retrievals using PLWP. The measurements were made between 2100 and 2400 UT (1300–1600 LT) on 17 September 2004 at the Barrow ARM site in conjunction with the Mixed-Phase Cloud Experiment (M-PACE) [*Verlinde et al.*, 2007]. This 3-h time period was chosen for the case study since only boundary layer clouds with a wide range of LWPs were present with no overlying cirrus or other cloud layers. The measurement site is located ~1–2 km inland, and the predominately grassy ground cover was largely senescent during the late summer study period. The ground temperature was ~3°C, and there was no evidence of ice particles in the clouds to complicate the retrieval of PLWP. The unbroken cloud deck and slowly changing radiances and LWPs measured by the MWR suggest that the clouds can be appropriately treated as homogeneous in the retrieval process. The wind was light ($3–6$ ms^{-1}) and from the South (160–200°). The ARM radar and ceilometer measurements show that the cloud deck lay between 0.5 and 1.1 km above ground level, rising slightly over the observation time. For September in the Arctic this is a typical cloud height and thickness [*Dong and Mace*, 2003b].

[15] For both retrieval methods the zenith-sky measurements are interpreted using a forward model based on the line-by-line radiative transfer code of *Portmann et al.* [2001]. This model incorporates the discrete ordinates radiative transfer model (DISORT) code [*Stamnes et al.*, 1988], and uses *Hu and Stamnes*'s [1993] parameterization to compute the optical properties of the cloud droplets. The measured quantities are compared to a look-up table containing the path enhancements and radiances calculated by the model for various values of the LWP, r_e, and solar zenith angle (SZA). The zenith radiance is computed by DISORT using 16 streams. The radiances are calculated with a solar forcing at the top of the model atmosphere of 4.77 $\times$ 10^{-2} Wm^{-2}/cm^{-1} at 500 nm. This value was obtained by convolving a measured solar spectrum [*Kurucz et al.*, 1984] with the filter function of our photodiode at 500 nm and adjusting for the Earth-Sun distance.

[16] The retrievals assume plane-parallel horizontally homogeneous clouds with a thickness of 600 m (0.5– 1.1 km in altitude) and a ground albedo of 0.1. Look-up tables were constructed with vertically varying LWC and r_e.
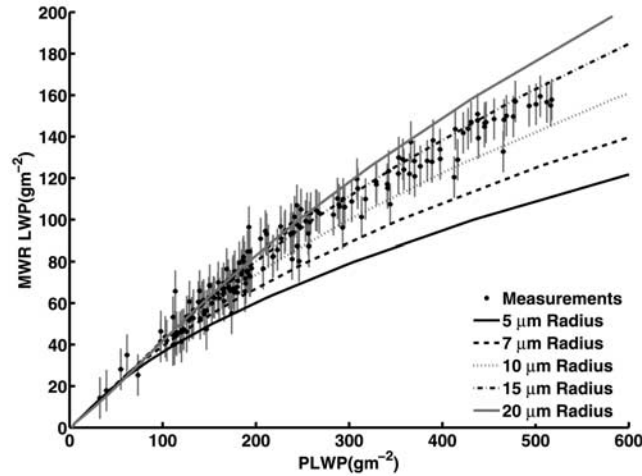
Figure 1. Measured NIR PLWP versus the MWR LWP observations for 17 September 2004, in Barrow, Alaska (69.5–76.3° SZA), and the look-up table curves of constant radii (5, 7, 10, 15, and 20 μm) for 70° SZA.

The cloud profiles of r_e and LWC were based on the reported profiles of *Morrison and Pinto* [2005]. The LWC was assumed to linearly increase from zero at the bottom of the cloud to a value at the top constrained by the integrated total LWP. The value of r_e is also assumed to increase linearly through the cloud with a value twice as large at the top as at the bottom (being constrained by its weighted mean).

[17] Both retrieval methods used a nonlinear, optimal estimation inversion [*Rodgers*, 2000] to iteratively determine the radius from the input parameters y given the errors in the measurement (S_ε) and errors in the prior knowledge of the desired retrieval parameters r_e (and LWP) (S_a):

$$x_{i+1} = x_a + \left(S_a^{-1} + K_i^T S_\varepsilon^{-1} K_i\right)^{-1} K_i^T S_\varepsilon^{-1} [y - F(x_i) + K_i(x_i - x_a)], \quad (2)$$

where x_a is the initial estimate of the retrieval parameters, x_i is the retrieved parameters for iteration i, F is the model calculation of the measured quantities, and K is the weighting function matrix (the sensitivity of the model calculated quantities to changes in the retrieval parameters). For the MWR-PLWP method, y is the path enhancement, given by the ratio PLWP/LWP. For the Rad$_{500}$-PLWP method, y consists of the radiance and PLWP observations. The retrieval is run as a function of the cosine of SZA and of $1/r$ to better linearize the retrieval of the radius. The difference between this optimal estimation inversion method and a direct interpolation (using cos SZA and $1/r$ radius interpolation of the radius) within the look-up table is small (<1%) for the cases examined here and for the measurement uncertainties assumed. Because the retrieval is run for cases in which the measurement fit does not improve with less constraint, the a priori uncertainty does not influence the resultant retrievals (or errors, since the retrieval errors in section 4 are almost entirely from measurement uncertainties). Nevertheless, this iterative

scheme is preferred to a simple interpolation scheme because it provides error information and retrieval characterization as described in section 4.

3.1. MWR-PLWP Retrieval of r_e

[18] The first method to retrieve r_e divides the PLWP from the NIR spectral measurements by the LWPs from the MWR measurements to obtain the path enhancement (often referred to as the air mass factor for trace gas retrievals) due to scattering by water droplets within the cloud. Measurements of NIR PLWP versus MWR LWP acquired during the case study period are displayed in Figure 1. The measurements are averaged over 1 min to align the MWR and NIR observations in time (MWR measurements were made every 20 s and NIR measurements were made every 30 s). Averaging over a longer time period could be desirable because of the different fields of view and cloud sample volume of the two sets of measurements [*Marshak et al.*, 1995; *Dong and Mace*, 2003a] (discussed further in section 4). Also displayed are the curves of constant radii for different path enhancements and radiances from the look-up table. The curves in Figure 1 correspond to the look-up table entries for 70° SZA used in the radius retrievals (the measurements range between 69.5 and 76.3° SZA). Error bars of 10 g m^{-2} for the MWR LWP are included to illustrate the significance of this relatively low-error estimate on the r_e retrievals. For small PLWPs the radii curves are close together, illustrating the reduced sensitivity of the path-enhancement to r_e. Thin cloud measurements provide insufficient independent pieces of information to accurately differentiate the radii for LWPs below ~100 g m^{-2} (see section 4.1).

[19] The data plotted in Figure 1 include an offset of −10 g m^{-2} applied to the MWR LWP to align the baselines of the two data sets, which demonstrated a clear bias that is not physically feasible (for a PLWP of zero the LWP should be also zero). This bias is well within the expected bias uncertainty for the ARM LWP retrievals of up to 30 g m^{-2} [*Marchand et al.*, 2003] and impacts the low-LWP radii retrievals much more than the higher-LWP radii because of the convergence of the radii curves. Note that while the offset was applied only to the LWP measurements here, some bias could also be present in the PLWP measurements. When the entire bias is assumed to be in PLWP (which we believe not to be the case, see discussion by *Turner et al.* [2007]), the retrieved r_e by this MWR-PLWP method increases by 7% (section 4.2).

[20] Error estimates used for the PLWP and MWR LWP (~8 and ~10 g m^{-2}, respectively) represent only the random error for these quantities after the 1-min temporal averages are made in the construction of the measurement covariance matrix S_ε. Systematic errors (biases) are assumed to be completely removed in the baseline alignment. Any systematic bias that changes with time (SZA) or LWP for either measurement is therefore not considered and would lead to an increase in the retrieved errors.

[21] The retrieved path enhancement matches the measured value with their error bars (Figure 2 top). Figure 2 middle shows the resulting effective radii for the MWR-PLWP retrieval. The root-mean-square RMS of the residuals from the measurement to model fit is 0.13 for all LWPs and 0.04 for LWPs > 100 g m^{-2} (33 and 16% of the path
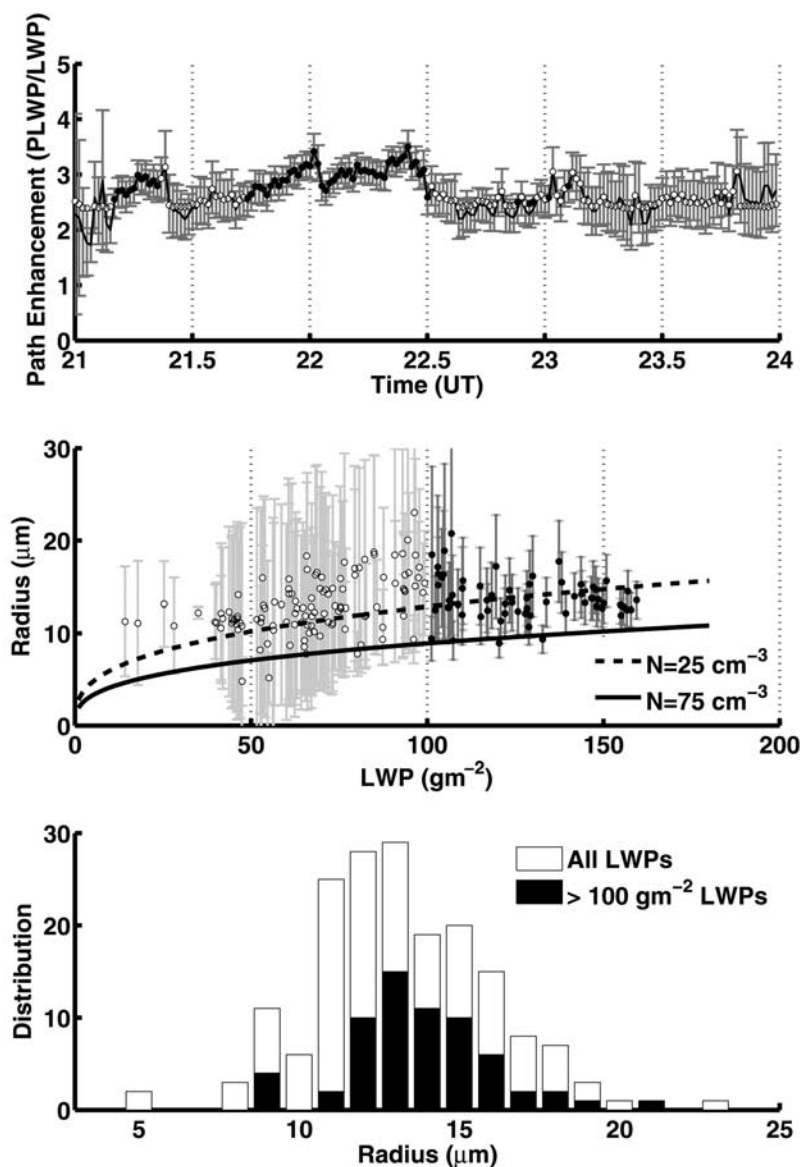
Figure 2. (top) Measured path enhancement (PLWP/LWP) (black curve with error bars) and retrieved fit (open circles) using the MWR-PWLP method. The solid circles correspond to those cases where the retrieved value is >100 g m^{-2}. (middle) Retrieved radii versus MWR LWP; the dashed and solid curves show the calculated radii for the indicated constant drop number densities. (bottom) Distribution of the retrieved radii, with a mean of 13.2 μm and a standard deviation of 2.8 μm.

enhancement error, respectively). For LWPs > 100 g m^{-2} the retrieved radii are consistent with the expected r_e from equation (1) when $N = 25$ cm^{-3} (the number density representative of the in situ measurements made near Barrow during M-PACE, see below) is assumed, along with $h = 600$ m and $\sigma_x = 0.31$ (the value used in the MMCR retrievals (see section 4.3)). For LWPs below 100 g m^{-2} the retrieved radii are slightly larger than given by equation (1) with $N = 25$ cm^{-3}, but agree within the errors. The retrieved effective radii for LWPs > 100 g m^{-2} have a mean of 13.8 μm and a standard deviation of 2.2 μm. For all LWPs the mean and standard deviation are 13.2 and 2.8 μm, respectively.

[22] Note that while $N = 25$ cm^{-3} is the number density representative of the in situ measurements made at Barrow during M-PACE (G. M. McFarquhar et al., Vertical variability of the phases, shapes, and size of hydrometeors in single layer mixed-phase Arctic stratus clouds, submitted to *Journal of the Atmospheric Sciences*, 2007, hereinafter referred to as McFarquhar et al., submitted manuscript, 2007), four flights in the region of Barrow found mean values of $N = 23, 26, 31$ and 52 cm^{-3} and a value of $N = 75$ cm^{-3} is used by default in the MMCR retrievals [*Shupe et al.*, 2005]. The N values of 25 and 75 cm^{-3} and the estimate of $\sigma_x = 0.31$, to be consistent with that used by the MMCR retrievals (see section 4.3), and $h = 600$ m are used
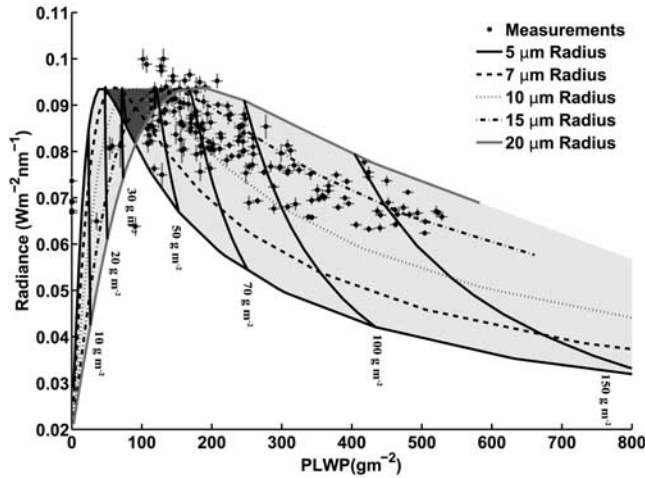
Figure 3. Absolute zenith radiances at 500 nm and PLWP observations shown with lines of constant radii and constant LWP for 70° SZA from the look-up table. The measurements must lie within the light gray area for the solution to be unique and feasible (radii within the range of 5–20 μm). The dark gray triangular region indicates where the radius/LWP retrieval corresponding to a given radiance and PLWP is double valued.

to calculate the r_e change with LWP from equation (1). However, the error bars shown in Figure 2 middle are too large to allow us to conclusively identify the presence of absence of such behavior in this data. The curves generated using equation (1) are not significantly sensitive to the assumed logarithm width; in the range of reasonable size distribution widths (0.2–0.5) these curves change by +0.5 to −2.5 μm from the nominal value.

3.2. Rad$_{500}$-PLWP Retrieval of r_e and LWP

[23] The second retrieval method combines the absolutely calibrated radiance at 500 nm with the NIR PLWP to obtain r_e and LWP. The radiances and PLWP observations for the Barrow study period are displayed in Figure 3. The look-up table of radiances and path enhancements for given values of SZA, LWP, and r_e were generated as detailed in section 3, and the forward model curves for constant radii and LWPs for a SZA of 70° are also displayed in Figure 3. The SZA, along with the ground albedo (to a much lesser extent), determines the maximum possible radiance for a constant radius when a plane-parallel cloud is assumed. The highest radiance measurements shown in Figure 3 occur for smaller SZAs, and thus the relevant look-up table curves are higher than those displayed for 70° SZA. For a given constant radius curve, increasing LWP increases the radiance seen at the ground until the path enhancement becomes large enough that the radiance begins to decrease because of attenuation. Thus the curves of constant radius are double valued with two PLWP values leading to the same radiance. The dark gray triangular region in Figure 3 shows the region where the retrieval of the LWP and radius is nonunique for plausible radii and thus cannot be used for retrieving these quantities by this method. The radii range is restricted in this case study to between 5 and 20 μm to limit the size of the dark gray area. For a given SZA and ground albedo we

assume that the measurement points need to lie in the area R given by the light gray shaded region for a realistic retrieval. This can be described as

$$R \in \left(\left(R_{\text{low}} \cup R_{\text{high}} \right) \notin \left(R_{\text{low}} \cap R_{\text{high}} \right) \right), \qquad (3)$$

where R_{low} is the area beneath the low-radius curve and R_{high} the area beneath the high-radius curve shown in Figure 3. R is the area given by the union of R_{low} and R_{high} excluding their intersection.

[24] Figure 3 illustrates that the LWP information is determined primarily by the PLWP measurements for low PLWPs (LWPs $< \sim$30 g m^{-2}). At higher PLWPs the radiance becomes more important for determining the LWP. This occurs because changes in LWP lead to larger changes in the cloud path enhancement under optically thicker clouds than they do under optically thinner ones. The radii retrievals rely upon the radiance and PLWP estimates under all conditions. For low LWPs ($<\sim$30 g m^{-2}) and for constant PLWP a decrease in radiance implies an increase in the radius, whereas at higher LWPs a decrease in the radiance is indicative of a smaller radius and larger cloud optical depths accompanied by greater cloud albedo. At very high PLWPs the radius retrieval becomes rather insensitive to the PLWP and depends primarily on the radiance value. We do not reach this limit in the analyses presented here.

[25] Similar to the MWR-PWLP retrieval only error estimates of the random errors of radiance and PLWP are considered ($\sim$0.005 Wm^{-2} nm^{-1} and 8 g m^{-2}, respectively) to construct S_ε. There is no bias applied to either of the measurements used in this method. This assumes that the intensity calibration does not introduce a bias in the radiance measurement and that the errors in the observations can be described as purely random errors for a 1-min temporal resolution. This is explored and discussed further in section 4.

[26] Figure 4 displays measurement fits for radiance and PLWP and the retrievals of r_e and LWP when the previously discussed selection criteria (equation (3)) is imposed upon the measurements. An a priori LWP of 20 or 100 g m^{-2} is used depending on whether the retrieval is in the low- or high-LWP regime, as indicated in Figure 3 (left/right light gray regions). The dependence upon the a priori values is low because of there being significant independent information in the PLWP and Rad$_{500}$ measurements (see section 4). A linear interpolation of $1/r$ and cos SZA is performed as in the MWR-PLWP retrieval to linearize the retrieval of the radius and LWP. Both the radiance and the PLWP measurements were well fitted by the retrieval. The RMS of the residuals of model fit to the radiance and PLWP measurements was 1.5 and 4.2% of the measurement errors, respectively. A mean r_e of 12.3 μm is retrieved with a standard deviation of 2.2 μm (mean = 13.6 μm, standard deviation = 1.9 μm for LWPs $>$ 100 g m^{-2}) consistent with the mid-September 2002 climatology for Barrow observed by *Dong and Mace* [2003b] of about 11 μm ($N \sim 100$ cm^{-3}) and with the mean retrieved by the MWR-PLWP method of 13.8 $\pm$ 2.2 μm. The retrieved LWP and r_e values follow the expected increase in r_e with LWP given by equation (1) ($h = 600$ m and $\sigma_x = 0.31$) and generally support the value

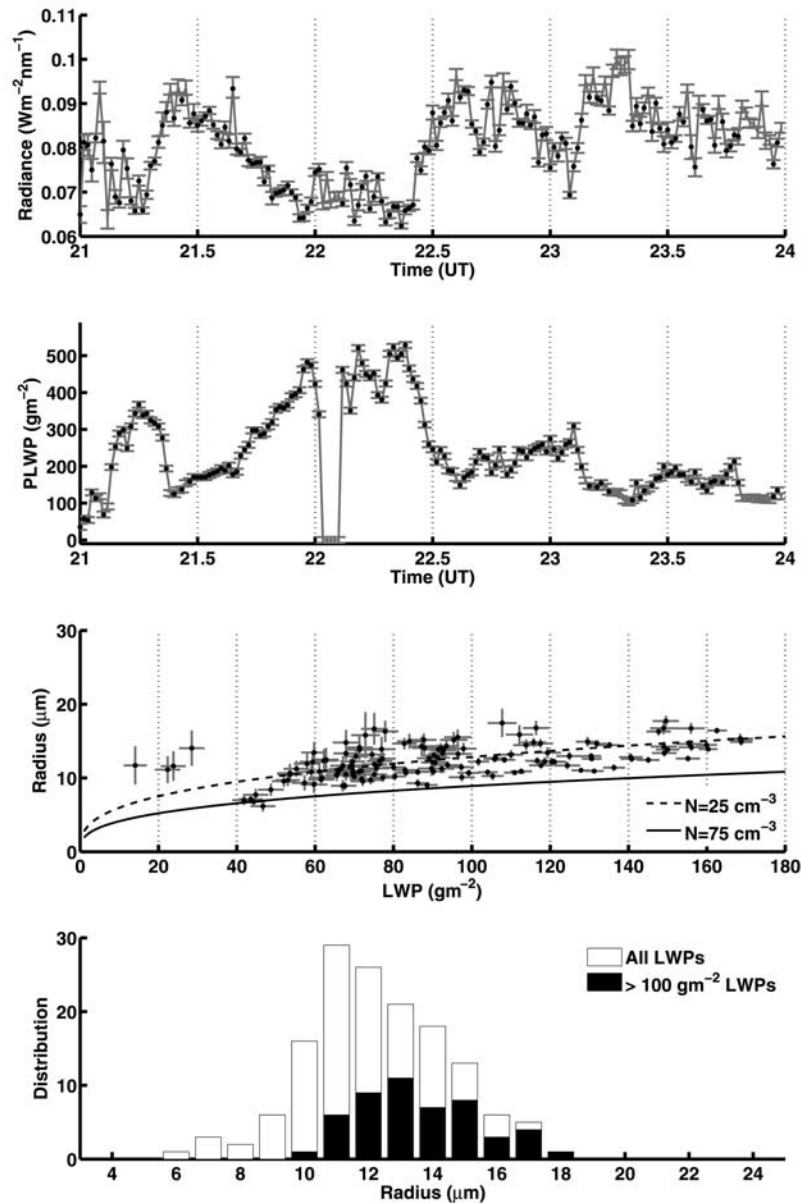**Figure 4.** Retrieval of the effective radius and LWP by the Rad_{500}-PWLP retrieval. (top) Radiance measurements at 500 nm (error bars) with the retrieved fit (solid circles). (top middle) PLWP measurements and retrieval fit. (bottom middle) Retrieved radii versus the retrieved LWPs, with the retrieval noise error given by the error bars and with the calculated radii assuming constant drop number densities. (bottom) Retrieved radius distribution with a mean of 12.3 μm with a standard deviation of 2.2 μm.

of $N \sim 25$ cm^{-3} seen by the M-PACE in situ measurements (although some of the larger radii support an even lower N). In section 4 the sensitivity of these retrievals to calibration and surface albedo is found to be relatively high. For operational implementation and future studies an accurate surface albedo and N would ideally be known.

4. Discussion

[27] A comparison of the radii retrieved using the MWR-PLWP and the Rad_{500}-PLWP retrievals is shown in Figure 5 left. The agreement between the radii retrieved using the two different methods is poor ($r^2 = 0.02$). The agreement is not significantly improved if the comparison is limited to LWPs > 100 g m^{-2} or if averaging is performed over a slightly longer time period (solid circles show 5-min averages). However, the good agreement of the mean values for the radii over the entire 3-h period is encouraging (i.e., Rad_{500}-PLWP, 13.6 $\pm$ 1.9 μm; MWR-PLWP, 13.8 $\pm$ 2.2 μm). While a different geometrical problem, this is consistent with the findings of *Dong and Mace* [2003a] that 30-min averages were required for good agreement between in situ aircraft and MWR-based r_e retrievals.
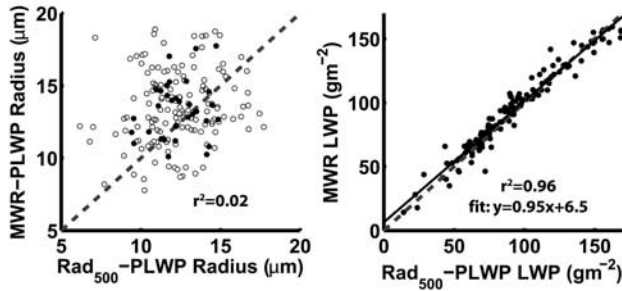
Figure 5. Comparison of radii and LWPs retrieved using the two methods described by this work. (left) Comparison of the radii retrieved by the MWR-PLWP and the Rad_{500}-PLWP methods (open circles). Solid circles are 5-min averaged results. (right) LWP retrieved by the Rad_{500}-PLWP and the MWR LWP measurements. The dashed line gives the 1:1 line.

[28] The sensitivity of the two radii retrieval methods examined in this case study to the clouds being sampled is clearly different, but the reason is not obvious. This may simply be a manifestation of the larger errors of the MWR-PLWP retrieval (section 4.1) or be due to sampling differences. Sampling differences result as the MWR emission is restricted to the zenith, while the PLWP and radiance quantities reflect absorption by a radiatively larger area of the cloud. The differences in sampling are compounded further by the different instrumental fields of view (4–5° for the MWR and 10° for the NIR and radiance measurements). Thus we would expect any differences due to three dimensional (3-D) horizontal cloud inhomogeneities to be reflected as differences in r_e and LWP between the MWR-PLWP and Rad_{500}-PLWP methods. However, the good agreement of the LWP values from the two methods (Figure 5 right) does not support horizontal cloud differences as being the cause of the poor r_e agreement. The correlation between the LWPs of the ARM MWR product and the Rad_{500}-PLWP retrieval is $r^2 = 0.96$ (slope of 0.95) at this 1-min resolution. Note that the MWR-LWP used in this correlation plot has the bias of 10 g m^{-2} already subtracted, while no bias was applied in the Rad_{500}-PLWP method. A y intercept of 6.5 is seen with the linear fit to MWR LWP versus Rad_{500}-PLWP LWP, indicating that the bias in the MWR-LWP may be larger than the assumed value of 10 g m^{-2}.

4.1. Errors and Uncertainties

[29] The uncertainties calculated for the values of r_e from the MWR-PLWP retrievals are shown Figure 6 left. These uncertainties follow directly from the measurement uncertainties of PLWP and LWP displayed in Figure 1 (formally the retrieval noise S_m [Rodgers, 2000]). The errors are the square root of the diagonal elements of the covariance matrix S_m, evaluated as

$$S_m = G_y S_\varepsilon G_y^T, \tag{4}$$

where G is the Gain matrix and evaluated as

$$G = \left(K^T S_\varepsilon^{-1} K + S_a^{-1}\right)^{-1} K^T S_\varepsilon^{-1}. \tag{5}$$

The diagonal elements of the averaging kernel matrix A ($A = GK$) give the degrees of freedom for signal, the number of independent pieces of information that can be retrieved from the measurements. Ideally, each element of the diagonal of A would be 1 if there is sufficient information contained within the measurements for its retrieval. It is critical to note that all errors and degrees of freedom for signal (number of independent pieces of information that can be retrieved from the measurements) are dependent upon the covariance assumptions. There may be further systematic or random uncertainties that have not been included in the observation uncertainties thus the retrieval errors and degrees of freedom reported in this section are typical of a best case retrieval. Forward model parameter errors (errors due to assumed model parameters, i.e., cloud height) and forward model errors (errors due to assumptions that approximate the true physics of the problem, i.e., homogeneous clouds) made in the forward model are discussed below in section 4.2.

[30] Figure 6 shows that for the MWR-PLWP retrieval the LWPs must be >100 g m^{N2} before the radii errors decrease to <6 μm and the independent pieces of information for signal is about 1. This is consistent with there being insufficient independent information contained within the path enhancement measurements to distinguish the radii when the LWP is below ~100 g m^{-2} (as shown in Figure 1 with the radii curves being very close together). This result is also consistent with the conclusions of *Min et al.* [2003] that the microwave LWP errors produce large errors in the radii retrieval for low LWPs when combined with MFRSR irradiance measurements. The errors found here in the MWR-PLWP retrieval are large since the quantity is the ratio of two measurements (resulting in larger errors in S_ε). Thus the evaluated uncertainties are greatly amplified.

[31] The errors and the degrees of freedom for signal in the Rad_{500}-PLWP retrieval of LWP and radii as a function of LWP are shown in Figure 7. The Rad_{500}-PLWP method has only slightly reduced sensitivity to the radii at smaller LWPs, compared to the large reduction seen with the MWR-PLWP retrieval. The associated radii errors from the PLWP and radiance errors are <3 μm almost everywhere. The precision of the radii with LWP is also clearly demonstrated in comparing the plots of radii versus LWP in Figures 2 and 4. The Rad_{500}-PLWP-retrieved LWP has ~1 independent piece of information for all LWPs and an uncertainty of
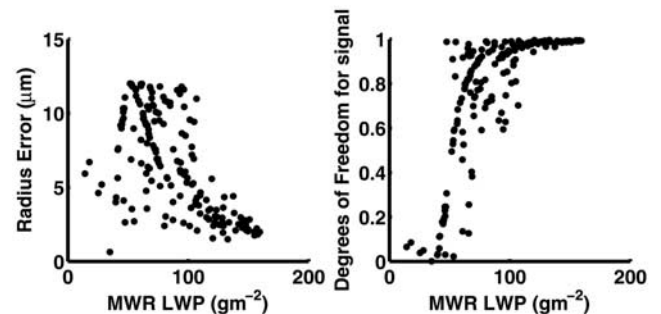

Figure 6. Errors and degrees of freedom for signal for the MWR-PLWP method. (left) Effective radii errors as a function of LWP. (right) Degrees of freedom for signal versus the LWP.
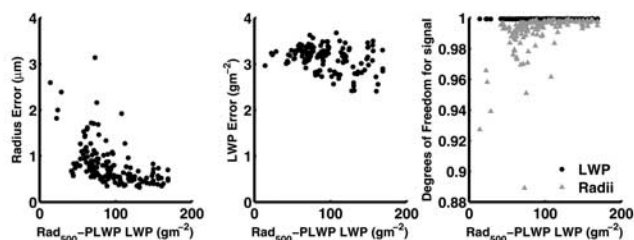
Figure 7. Error for retrievals of (left) r_e and (middle) LWP for the Rad_{500}-PLWP retrieval. (right) Degrees of freedom for signal for the LWP (gray triangles) and radius (solid circles) retrievals.

<4 g m^{-2}. As discussed in section 3.2, the PLWP provides information of the LWP independent of radiance for low LWPs (Figure 3 left). If these low-PLWP measurements (thus low LWPs) were combined with measurements with a higher sensitivity to radii than the radiance measurements used here, retrievals with smaller errors at low LWPs would be possible.

4.2. Forward Model Assumptions and Sensitivities

[32] As noted in section 3, the forward model assumes plane-parallel horizontally homogeneous clouds with a thickness of 600 m at a height of 0.5–1.1 km, a logarithm normal size droplet distribution, and a ground albedo of 0.1. The sensitivity of the retrieved parameters to large changes in cloud height (+3 km) and thickness (1/2) are given in Table 1. The effects of both cloud height and thickness on the MWR-PLWP radii retrievals are seen to be negligible ($<1\%$). The radii retrievals for the Rad_{500}-PLWP method are more sensitive, increasing by 6%, if the clouds were assumed to be 3 km higher. While the ceilometer data do show some increase in clouds height over the study period, it is much <3 km and the effects of errors in the assumed cloud thickness and height can be neglected. This is not surprising since it is the amount of liquid water in the cloud and the number of scattering events that provide most of the information contained within the PLWP observations.

[33] *Wendisch et al.* [2004] report surface albedos over land between 0.02 and 0.09 at 500 nm and between 0.2 and 0.3 in the PLWP spectral region. The sensitivity of the model to our assumed value of 0.1 is also shown in Table 1. A decrease in ground albedo from 0.1 to 0.0 at 500 nm increases the retrieved radii by 16% and LWPs by 6% for the Rad_{500}-PLWP method. Increasing the 1400 nm albedo to 0.3, decreases both the retrieved radii and LWP by 7%. Smaller r_e and LWP retrievals result for the Rad_{500}-PLWP method with increases in albedo because of increases in both the radiance and PLWP model curves relative to the given radiance and PLWP observations (see Figure 3). Conversely, an increase in surface albedo results in larger r_e retrievals for the MWR-PLWP method because of an increase in the model PLWP for a given LWP (see Figure 1). The MFR and MFRSR measurements at Barrow support an albedo of $\sim$0.1 at 500 nm, but the albedo at 1400 nm is unknown for this case study. This sensitivity to the albedo could be avoided with a routine measure of the ground albedo specifically made at 500 and 1400 nm (0.9–1.7 μm PLWP spectral range) to reduce this source of error and improve these retrievals in future.

[34] The logarithm size distribution assumption is expected to produce a negligible error as discussed by *Hu and Stamnes* [1993]. A reasonable size distribution with the same r_e produces essentially identical optical liquid cloud properties over a much wider wavelength range than is considered in this study.

[35] The sensitivity of the Rad_{500}-PLWP retrieval to a 5% change in the calibration of the absolute radiances results in a larger change in the mean radii ($\sim$16%) relative to mean change in LWP ($\sim$4%) for the Rad_{500}-PLWP retrieval. The resultant change is somewhat dependent on the LWP (i.e., at 60 g m^{-2} $\sim$20% and at 170 g m^{-2} $\sim$11%). If we assume that a bias of +25 g m^{-2} exists in the PLWP observations, mean values for both the radii and LWPs increase by $\sim$12% for the Rad_{500}-PLWP method. For the MWR-PLWP retrieval, if we assume a +25 g m^{-2} bias in the PLWP (instead of -10 g m^{-2} in the MWR) a +7% increase in the radii is retrieved. While we believe we have avoided these observation based error influences in our retrievals [*Turner et al.*, 2007], it is useful to note the sensitivity to the calibration and potential biases.

[36] The sensitivity of our retrievals to the vertical cloud LWC profile shape was probed. When a constant profile of LWC is assumed for the modeled cloud, the retrieved radii are only slightly affected, however, the LWP retrieval is increased by 4%. The forward model error due to horizontal cloud inhomogeneities is more difficult to probe without examining the realistic cloud fields in a 3-D cloud model. In an inhomogeneous cloud case, radiances would change rapidly, our smoothly changing radiance measurements provides some evidence that in this case study we have a

Table 1. Sensitivity to Forward Model Parameter Assumptions and for Comparison the Retrieval Error Derived Primarily From the Observational Errors

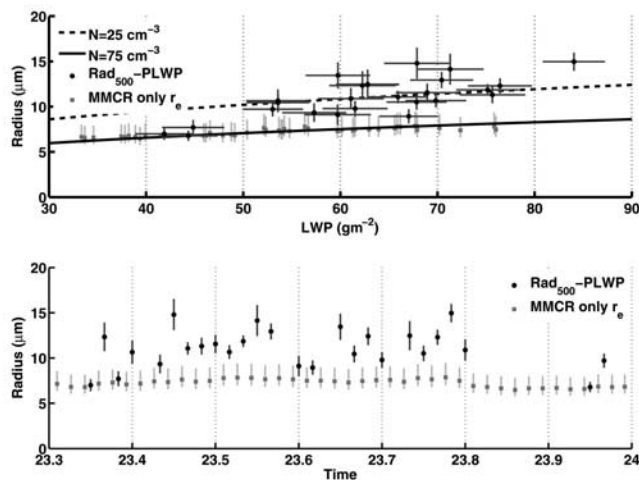|	MWR-PLWP Radius, %	Rad_{500}-PLWP Radius, %	Rad_{500}-PLWP LWP, %
Cloud height ($\sim$3 km higher)	+0.2	+6	+0.1
Cloud thickness (halved)	+0.01	-1.3	-0.3
Ground albedo (500 nm; 0.0)	...	+16	+6
Ground albedo (1400 nm; 0.3)	+18	-7	-7
Radiance calibration (+/-5%)	...	+16/-12	+4/-3
PLWP bias (+25 g m^{-2})	+7	+11	+12
Constant LWC cloud profile assumed	-1.7	0.4	4
Retrieval error			
Observation only	49	7	4
LWP >100 g m^{-2}	25	7	4

Figure 8. Comparison of radii retrieved using the Rad_{500}-PLWP method and the LWC-weighted mean r_e values retrieved using the MMCR empirical method [*Shupe et al.*, 2001; *Frisch et al.*, 2002] assuming $N = 75$ cm^{-3} and $\sigma_x = 0.31$. The error range given on the MMCR r_e values show the retrieved values when 25 and 150 cm^{-3} are assumed for N.

relatively homogeneous cloud scene. As discussed in section 4, with Figure 5 we expect that cloud inhomogeneities would cause most problems in the MWR-PLWP retrieval. However, we also expect that both the LWPs and r_e retrieved would be affected in the Rad_{500}-PLWP method by inhomogeneous clouds. Thus, for a comparison of r_e and LWP (Figure 5) estimated from the MWR-PLWP and Rad_{500}-PLWP methods we would expect both comparisons to be poor if cloud inhomogeneities were the cause. While in Figure 5 we find that the r_e comparison to be poor, the LWP is very good, leading us to logically conclude that cloud inhomogeneities are not the primary source of error.

4.3. MMCR Comparison

[37] The MMCR derives both r_e and LWC profiles using radar reflectivity signals. For this comparison the empirical rather than the MWR LWP based MMCR retrieval method is used. The empirical MMCR retrieval method bases the r_e on a radar reflectivity power law relationship, assuming fixed and constant values for both the droplet concentration ($N = 75$ cm^{-3}) and the logarithmic width ($\sigma_x = 0.31$) of a lognormal droplet size distribution. The MMCR empirical r_e retrieval is not very sensitive to σ_x but is more sensitive to the assumed value of N [*Frisch et al.*, 2002; *Shupe et al.*, 2005].

[38] In Figure 8 we compare the effective radii retrieved by the Rad_{500}-PLWP method with those retrieved by the MMCR. The values retrieved by the MWR-PLWP method are not shown, as the comparison is limited to LWPs below 100 g m^{-2}. There was only a limited time within the 3-h period when the MMCR radii retrieval was unaffected by drizzle and/or ice crystal precipitation (low-LWP clouds, 2318–2400 UT), and the comparison is restricted to this interval (the radar r_e retrievals are affected by large (drizzle) particles dominating the radar signal). Neither the PLWP nor the Rad_{500} measurements appear to be influenced by the

presence of drizzle. To directly compare the radar results with the values of r_e retrieved by the Rad_{500}-PLWP method, we evaluate the LWC-weighted mean r_e value for the MMCR.

[39] The r_e values from the Rad_{500}-PLWP retrieval for this time (mean of 11.0 μm, standard deviation of 2.1 μm) are significantly higher than the MMCR values (mean of 7.2 μm, standard deviation of 0.4 μm). Reasons for this discrepancy are as yet unclear but possibilities include differences in the fields of view, an assumed value of the surface albedo that is too low (see section 4.2), or errors in the assumed value of N. We note that the LWC-weighted mean r_e values from the MMCR empirical retrieval lie exactly on the expected curve given by equation (1) (assuming $N = 75$ cm^{-3}, $\sigma_x = 0.31$ and $h = 600$ m). While $N = 75$ cm^{-3} was assumed in the MMCR analysis, the M-PACE aircraft data support a smaller value of $N \sim 25$ cm^{-3} (McFarquhar et al., submitted manuscript, 2007). The calculated line for $N = 25$ cm^{-3} from equation (1) is significantly higher and more consistent with the Rad_{500}-PLWP results. However, the values of r_e are not dramatically changed when $N = 25$ cm^{-3} is assumed in the MMCR retrieval (shown by the upper limit of the MMCR error bars). For future comparisons it would be desirable to have coincident (in time and space) in situ N and surface albedo measurements so that a more quantitative verification could be obtained, thus enabling the exact identification of the cause of the discrepancy (i.e., observational (different sampling) or model (assumptions in r_e retrievals)).

5. Conclusions and Outlook

[40] Two new methodologies for the retrieval of cloud droplet effective radius r_e using ground-based near-infrared measurements of liquid water absorption have been described in this paper. The first method (MWR-PLWP) combines collocated MWR measurements of LWP with our retrieved values of PLWP to estimate r_e from the inferred path enhancement, i.e., PLWP/LWP. The second method (Rad_{500}-PLWP) combines the retrieved values of PLWP with radiance measurements at 500 nm to simultaneously retrieve r_e and LWP without using the MWR measurements. Both methods are illustrated in a case study with observations made at Barrow, Alaska, on 17 September 2004.

[41] The MWR-PLWP method is a relatively uncomplicated means of deriving r_e for LWP > 100 gm^{-2}, but the sensitivity to r_e decreases significantly for smaller LWPs. This leads to errors in excess of 6 μm at low LWP and PLWP where the path enhancement ratio (PLWP/LWP) approaches 1. The overall accuracy is also limited by uncertainties in the MWR LWP measurements, and we therefore conclude that the MWR-PLWP method is not currently a viable technique for routinely retrieving r_e for the range of LWPs considered in this study.

[42] In contrast, the Rad_{500}-PLWP provides good r_e and LWP products with reasonably low errors and is a viable means for remote sensing of horizontally homogeneous clouds from the ground. Hence this method is suitable for studies of the indirect aerosol effect when combined with additional aerosol measurements. The Rad_{500}-PLWP methodology avoids the influence of any MWR LWP errors or

bias on the retrieved radii and is characterized by errors ~ 3 μm ($\sim 23\%$), that is in the order of the errors seen by the methods described by *Min and Harrison* [1996] and *Min et al.* [2003]. Complications due to different fields of view, sampling radiatively different cloud areas, and different temporal resolution are avoided, thus providing an independent LWP measure with small error ~ 4 μm (4%). For LWPs $< \sim 25$ g m^{-2} or $> \sim 50$ g m^{-2}, with the precise ranges depending on r_e, the Rad$_{500}$-PLWP method retrieves good information about the r_e and LWP. The forward modeling parameter error of albedo and the calibration errors are the greatest source of retrieval errors (other than the measurement errors) for both methods contributing potentially $\sim 18\%$. The LWPs derived using the Rad$_{500}$-PLWP retrieval and the ARM MWR LWP product agree with an $r^2 = 0.96$ and slope of 0.95. Comparison with the radii retrieved by the MWR-PLWP method and the Rad$_{500}$-PLWP shows significant disagreement, although the mean r_e values (LWP > 100 gm^{-2}) for the 3-h case study do agree well.

[43] The comparison with MMCR, while limited to LWPs below 100 g m^{-2} showed the Rad$_{500}$-PLWP method to retrieve higher r_e than the LWC-weighted mean r_e of the MMCR. The Rad$_{500}$-PLWP r_e values are consistent (within errors) with the calculated r_e given N of 25 cm^{-3} (M-PACE measurements), the logarithm width consistent with the MMCR retrievals and $h = 600$ m. The MMCR-retrieved r_e are also internally consistent with an N of 75 cm^{-3}, and using a value of $N = 25$ cm^{-3}, does not bring these two methods into full agreement. The reasons for this difference of ~ 3 μm between the r_e retrievals are not resolved here and would require a longer, more detailed study in the future. Possible explanations include differences in field of view, a higher surface albedo decreasing the Rad$_{500}$-PLWP r_e retrieval, or some other observational uncertainty. An independent in situ estimate of N would be valuable for future intercomparison studies.

[44] Theoretically, the PLWP, Rad$_{500}$, and LWP measurements could be all combined in an optimal estimation framework, but the information gain would not be large because of the MWR LWP measurement already being a retrieval product of the Rad$_{500}$-PLWP method. Ideally, one would work directly with the brightness temperatures from the MWR. One could therefore take advantage of the complication of a different field of view from the MWR to obtain information on the radiative smoothing or cloud inhomogeneities once the MWR errors are smaller and the issue of bias is removed, i.e., with the next generation of multichannel microwave sensors.

References

Boers, R., J. R. Acarreta, and J. L. Gras (2006), Satellite monitoring of the first indirect aerosol effect: Retrieval of the droplet concentration of water clouds, *J. Geophys. Res.*, *111*, D22208, doi:10.1029/2005JD006838.

Charlson, R. J., S. E. Schwartz, J. M. Hales, R. D. Cess, J. A. Coakley Jr., J. E. Hansen, and D. J. Hofmann (1992), Climate forcing by anthropogenic aerosols, *Science*, *255*(5043), 423–430.

Crewell, S., and U. Löhnert (2003), Accuracy of cloud liquid water path from ground-based microwave radiometry: 2. Sensor accuracy and synergy, *Radio Sci.*, *38*(3), 8042, doi:10.1029/2002RS002634.

Daniel, J. S., R. W. Portmann, H. L. Miller, S. Solomon, A. O. Langford, C. S. Eubank, R. Schofield, D. D. Turner, and M. D. Shupe (2006), Cloud property estimates from zenith spectral measurements of scattered sunlight between 0.9 and 1.7 μm, *J. Geophys. Res.*, *111*, D16208, doi:10.1029/2005JD006641.

Dong, X. Q., and G. G. Mace (2003a), Profiles of low-level stratus cloud microphysics deduced from ground-based measurements, *J. Atmos. Oceanic Technol.*, *20*(1), 42–53.

Dong, X. Q., and G. G. Mace (2003b), Arctic stratus cloud properties and radiative forcing derived from ground-based data collected at Barrow, Alaska, *J. Clim.*, *16*(3), 445–461.

Feingold, G., R. Furrer, P. Pilewskie, L. A. Remer, Q. Min, and H. Jonsson (2006), Aerosol indirect effect studies at Southern Great Plains during the May 2003 Intensive Operations Period, *J. Geophys. Res.*, *111*, D05S14, doi:10.1029/2004JD005648.

Frisch, A. S., G. Feingold, C. W. Fairall, T. Uttal, and J. B. Snider (1998), On cloud radar and microwave radiometer measurements of stratus cloud liquid water profiles, *J. Geophys. Res.*, *103*(D18), 23,195–23,198.

Frisch, S., M. Shupe, I. Djalalova, and M. Poellot (2002), The retrieval of stratus cloud droplet effective radius with cloud radars, *J. Atmos. Oceanic Technol.*, *19*(6), 835–842.

Gao, B., and Y. J. Kaufman (2003), Water vapor retrievals using Moderate Resolution Imaging Spectroradiometer (MODIS) near-infrared channels, *J. Geophys. Res.*, *108*(D13), 4389, doi:10.1029/2002JD003023.

Garrett, T. J., C. Zhao, X. Dong, G. G. Mace, and P. V. Hobbs (2004), Effects of varying aerosol regimes on low-level Arctic stratus, *Geophys. Res. Lett.*, *31*, L17105, doi:10.1029/2004GL019928.

Han, Q., W. B. Rossow, J. Chou, and R. M. Welch (1998), Global survey of the relationships of cloud albedo and liquid water path with droplet size using ISCCP, *J. Clim.*, *11*(7), 1516–1528.

Harrison, L., and J. Michalsky (1994), Objective algorithms for the retrieval of optical depths from ground-based measurements, *Appl. Opt.*, *33*(22), 5126–5132.

Harrison, L., J. Michalsky, and J. Berndt (1994), Automated multifilter rotating shadow-band radiometer: An instrument for optical depth and radiation measurements, *Appl. Opt.*, *33*(22), 5118–5125.

Hogg, D. C., M. T. Decker, F. O. Guiraud, K. B. Earnshaw, D. A. Merritt, K. P. Moran, W. B. Sweezy, R. G. Strauch, E. R. Westwater, and C. G. Little (1983), An automatic profiler of the temperature, wind and humidity in the troposphere, *J. Clim. Appl. Meteorol.*, *22*(5), 807–831.

Hu, Y. X., and K. Stamnes (1993), An accurate parameterization of the radiative properties of water clouds suitable for use in climate models, *J. Clim.*, *6*(4), 728–742.

Intergovernmental Panel on Climate Change (2001), *Climate Change 2001: Synthesis Report: Contribution of Working Groups I, II and III to the Third Assessment Report of the Intergovernmental Panel on Climate Change*, edited by R. T. Watson et al., Cambridge Univ. Press, Cambridge, U. K.

Kim, B.-G., S. E. Schwartz, M. A. Miller, and Q. Min (2003), Effective radius of cloud droplets by ground-based remote sensing: Relationship to aerosol, *J. Geophys. Res.*, *108*(D23), 4740, doi:10.1029/2003JD003721.

Kou, L. H., D. Labrie, and P. Chylek (1993), Refractive indexes of water and ice in the 0.65 to 2.5 μm spectral range, *Appl. Opt.*, *32*(19), 3531–3540.

Kurucz, R. L., et al. (1984), *Solar Flux Atlas From 296 to 1300 nm*, 2 ed., 240 pp., Natl. Sol. Obs. Atlas, Sunspot, New Mexico.

Langford, A. O., R. W. Portmann, J. S. Daniel, H. L. Miller, C. S. Eubank, S. Solomon, and E. G. Dutton (2005), Retrieval of ice crystal effective diameters from ground-based near-infrared spectra of optically thin cirrus, *J. Geophys. Res.*, *110*, D22201, doi:10.1029/2005JD005761.

Liljegren, J. C., and B. M. Lesht (1996), Measurements of integrated water vapor and cloud liquid water from microwave radiometers at the DOE ARM cloud and radiation test bed in the U.S. Southern Great Plains, paper presented at International Geoscience and Remote Sensing Symposium, Inst. of Electr. and Electr. Eng., Inc., Lincoln, Nebr.

Marchand, R., T. Ackerman, E. R. Westwater, S. A. Clough, K. Cady-Pereira, and J. C. Liljegren (2003), An assessment of microwave absorption models and retrievals of cloud liquid water using clear-sky data, *J. Geophys. Res.*, *108*(D24), 4773, doi:10.1029/2003JD003843.

Marshak, A., A. Davis, W. Wiscombe, and R. Cahalan (1995), Radiative smoothing in fractal clouds, *J. Geophys. Res.*, *100*(D12), 26,247–26,262.

McFarlane, S. A., K. F. Evans, and A. S. Ackerman (2002), A Bayesian algorithm for the retrieval of liquid water cloud properties from microwave radiometer and millimeter radar data, *J. Geophys. Res.*, *107*(D16), 4317, doi:10.1029/2001JD001011.

Miles, N. L., J. Verlinde, and E. E. Clothiaux (2000), Cloud droplet size distributions in low-level stratiform clouds, *J. Atmos. Sci.*, *57*(2), 295–311.

Min, Q., and M. Duan (2005), Simultaneously retrieving cloud optical depth and effective radius for optically thin clouds, *J. Geophys. Res.*, *110*, D21201, doi:10.1029/2005JD006136.

Min, Q., and L. C. Harrison (1996), Cloud properties derived from surface MFRSR measurements and comparison with GOES results at the ARM SGP site, *Geophys. Res. Lett.*, *23*(13), 1641–1644.

Min, Q.-L., M. Duan, and R. Marchand (2003), Validation of surface retrieved cloud optical properties with in situ measurements at the Atmospheric Radiation Measurement Program (ARM) South Great Plains site, *J. Geophys. Res.*, *108*(D17), 4547, doi:10.1029/2003JD003385.

Moran, K. P., B. E. Martner, M. J. Post, R. A. Kropfli, D. C. Welsh, and K. B. Widner (1998), An unattended cloud-profiling radar for use in climate research, *Bull. Am. Meteorol. Soc.*, *79*(3), 443–455.

Morris, V. R. (2006), Microwave radiometer (MWR) handbook, *ARM Tech. Rep. TR-016*, 19 pp., U.S. Dep. of Energy, Off. of Sci., Off. of Biol. and Environ, Res., Washington, D. C. (Available at http://www.arm.gov/publications/tech_reports/handbooks/mwr_handbook.pdf)

Morrison, H., and J. O. Pinto (2005), Mesoscale modeling of springtime Arctic mixed-phase stratiform clouds using a new two-moment bulk microphysics scheme, *J. Atmos. Sci.*, *62*(10), 3683–3704.

Noxon, J. F. (1975), Nitrogen dioxide in the stratosphere and troposphere measured by ground-based absorption spectroscopy, *Science*, *189*(4202), 547–549.

Pilewskie, P., J. Pommier, R. Bergstrom, W. Gore, S. Howard, M. Rabbette, B. Schmid, P. V. Hobbs, and S. C. Tsay (2003), Solar spectral radiative forcing during the Southern African Regional Science Initiative, *J. Geophys. Res.*, *108*(D13), 8486, doi:10.1029/2002JD002411.

Platt, U. (1994), Differential optical absorption spectroscopy (DOAS), in *Air Monitoring by Spectroscopic Techniques*, edited by M. W. Sigrist, pp. 27–76, John Wiley, New York.

Portmann, R. W., S. Solomon, R. W. Sanders, J. S. Daniel, and E. G. Dutton (2001), Cloud modulation of zenith sky oxygen photon path lengths over Boulder, Colorado: Measurement versus model, *J. Geophys. Res.*, *106*(D1), 1139–1156.

Rodgers, C. D. (2000), *Inverse Methods for Atmospheric Sounding: Theory and Practice*, 1st ed., 238 pp., World Sci., Singapore.

Shupe, M. D., T. Uttal, S. Y. Matrosov, and A. S. Frisch (2001), Cloud water contents and hydrometeor sizes during the FIRE Arctic Clouds Experiment, *J. Geophys. Res.*, *106*(D14), 15,015–15,028.

Shupe, M. D., T. Uttal, and S. Y. Matrosov (2005), Arctic cloud microphysics retrievals from surface-based remote sensors at SHEBA, *J. Appl. Meteorol.*, *44*(10), 1544–1562.

Stamnes, K., S.-C. Tsay, W. Wiscombe, and K. Jayaweera (1988), Numerically stable algorithm for discrete-ordinate-method radiative-transfer in multiple-scattering and emitting layered media, *Appl. Opt.*, *27*(12), 2502–2509.

Turner, D. D., et al. (2007), Retrieving liquid water path and precipitable water vapor from the Atmospheric Radiation Measurement (ARM) microwave radiometers, *IEEE Trans. Geosci. Remote Sens.*, in press.

Twomey, S. (1974), Pollution and planetary albedo, *Atmos. Environ.*, *8*(12), 1251–1256.

Verlinde, J., et al. (2007), The mixed-phase Arctic cloud experiment, *Bull. Am. Meteorol. Soc.*, *88*(2), 205–221.

Warren, S. G., C. J. Hahn, and J. London (1985), Simultaneous occurrence of different cloud types, *J. Clim. Appl. Meteorol.*, *24*(7), 658–667.

Wendisch, M., P. Pilewskie, E. Jäkel, S. Schmidt, J. Pommier, S. Howard, H. H. Jonsson, H. Guan, M. Schröder, and B. Mayer (2004), Airborne measurements of a real spectral surface albedo over different sea and land surfaces, *J. Geophys. Res.*, *109*, D08203, doi:10.1029/2003JD004392.

Westwater, E. R. (1978), Accuracy of water-vapor and cloud liquid determination by dual-frequency ground-based microwave radiometry, *Radio Sci.*, *13*(4), 677–685.

Westwater, E. R. (1993), *Ground-Based Microwave Remote Sensing of Meteorological Variables*, pp.145–213, John Wiley, New York.

————————————

J. S. Daniel, C. S. Eubank, A. O. Langford, M. L. Melamed, H. L. Miller, R. W. Portmann, and S. Solomon, NOAA, Chemical Sciences Division, Earth Systems Research Laboratory, 325 Broadway Street, Boulder, CO 80305, USA.

R. Schofield, Alfred Wegener Institute for Polar and Marine Research, P.O. Box 60 01 49, D-14401 Potsdam, Germany. (robyn.schofield@gmail.com)

M. D. Shupe, Cooperative Institute for Research in Environmental Sciences, University of Colorado, Boulder, CO 80309, USA.

D. D. Turner, Space Science and Engineering Center, University of Wisconsin-Madison, Madison, WI 53706, USA.